JPn Neuroscience
The Journal of Physiology
J Physiol 594.13 (2016) pp 3729–3744

The transcription factor NeuroD2 coordinates synaptic innervation and cell intrinsic properties to control excitability of cortical pyramidal neurons

Fading Chen[1], Jacqueline T. Moran[2], Yihui Zhang[1], Kristin M. Ates[1,2], Diankun Yu[1], Laura A. Schrader[1,2], Partha M. Das[1], Frank E. Jones[1] and Benjamin J. Hall[1,2,3]

[1] *Department of Cell and Molecular Biology, School of Science and Engineering, Tulane University, New Orleans, LA 70118, USA*
[2] *The Neuroscience Program, School of Science and Engineering, Tulane University, New Orleans, LA 70118, USA*
[3] *Neuroscience, Ophthalmology and Rare Diseases, F. Hoffmann-La Roche, Basel Innovation Centre, Basel 4070, Switzerland*

Key points

- Synaptic excitation and inhibition must be properly balanced in individual neurons and neuronal networks to allow proper brain function.
- Disrupting this balance may lead to autism spectral disorders and epilepsy.
- We show the basic helix–loop–helix transcription factor NeuroD2 promotes inhibitory synaptic drive but also decreases cell-intrinsic neuronal excitability of cortical pyramidal neurons both *in vitro* and *in vivo*.
- We identify two genes potentially downstream of NeuroD2-mediated transcription that regulate these parameters: gastrin-releasing peptide and the small conductance, calcium-activated potassium channel, SK2.
- Our results reveal an important function for NeuroD2 in balancing synaptic neurotransmission and intrinsic excitability.
- Our results offer insight into how synaptic innervation and intrinsic excitability are coordinated during cortical development.

Abstract Synaptic excitation and inhibition must be properly balanced in individual neurons and neuronal networks for proper brain function. Disruption of this balance during development may lead to autism spectral disorders and epilepsy. Synaptic excitation is counterbalanced by synaptic inhibition but also by attenuation of cell-intrinsic neuronal excitability. To maintain proper excitation levels during development, neurons must sense activity over time and regulate the expression of genes that control these parameters. While this is a critical process, little is known about the transcription factors involved in coordinating gene expression to control excitatory/inhibitory synaptic balance. We show here that the basic helix–loop–helix transcription factor NeuroD2 promotes inhibitory synaptic drive but also decreases cell-intrinsic neuronal excitability of cortical pyramidal neurons both *in vitro* and *in vivo* as shown by *ex vivo* analysis of a NeuroD2 knockout mouse. Using microarray analysis and comparing wild-type and NeuroD2 knockout cortical networks, we identified two potential gene targets of NeuroD2 that contribute to these processes: gastrin-releasing peptide (GRP) and the small conductance, calcium-activated potassium channel, SK2. We found that the GRP receptor antagonist RC-3059 and the SK2 specific blocker apamin partially reversed the effects of increased NeuroD2 expression on inhibitory synaptic drive and action potential repolarization, respectively. Our results reveal an important

© 2016 The Authors. The Journal of Physiology © 2016 The Physiological Society
DOI: 10.1113/JP271953

function for NeuroD2 in balancing synaptic neurotransmission and intrinsic excitability and offer insight into how these processes are coordinated during cortical development.

(Resubmitted 19 January 2016; accepted after revision 13 April 2016; first published online 5 May 2016)
Corresponding author B. Hall: F. Hoffmann-La Roche Ltd, Bldg 70 Rm 411, Grenzacherstrasse 124, 4070 Basel, Switzerland. Email: benjamin.hall@roche.com

Abbreviations AP, action potential; AHP, afterhyperpolarization; E/I, excitatory/inhibitory; GRP, gastrin-releasing peptide; GRPR, gastrin-releasing peptide receptor; IEI, inter-event interval; mEPSC, miniature excitatory postsynaptic current; mIPSC, miniature inhibitory postsynaptic current; NeuroD2, neurogenic differentiation factor 2; sEPSC, spontaneous excitatory postsynaptic current; sIPSC, spontaneous inhibitory postsynaptic current; TF, transcription factor.

Introduction

Alterations in cortical circuit development can lead to neurodevelopmental disorders including autism spectral disorders and epilepsy (Hoischen *et al.* 2014; Lee *et al.* 2015). Proper neuronal circuit formation and function require coordination between excitatory and inhibitory synaptic innervation as well as the cell-intrinsic excitability of individual neurons (Turrigiano, 2011). This means that individual neurons must sense and integrate synaptic activity over time and correspondingly control expression of genes regulating synaptic innervation and intrinsic excitability. While the transcription factors (TFs) that control the initial fating of neuronal cell types are well defined (Kohwi & Doe, 2013; Imayoshi & Kageyama, 2014), the TFs and downstream genes that coordinate neuronal excitability and synaptic connectivity during circuit formation, after neuronal cell fating, are less well understood.

Neurogenic differentiation factor 2 (NeuroD2) is a highly conserved TF of the basic helix–loop–helix protein family and is one of the first TFs expressed in post-mitotic neurons (McCormick *et al.* 1996). NeuroD2 trans-activation can be activated by calcium influx making it a good candidate for linking neuronal activity to the transcription of genes that regulate synaptic innervation and intrinsic excitability in developing neurons. It is well established that NeuroD2 promotes neuronal survival and excitatory synapse maturation (Olson *et al.* 2001; Ince-Dunn *et al.* 2006; Wilke *et al.* 2012). However, its role in regulating inhibitory synapse development and intrinsic neuronal excitability has not been examined. Furthermore, the direct targets of this important late-stage TF are largely unknown in post-mitotic neurons.

We examined the role of NeuroD2 using gene knockdown and knockout (KO), and overexpression while measuring synaptic innervation and intrinsic excitability of pyramidal neurons in developing cortical networks both *in vitro* and *ex vivo*. In parallel, we performed microarray analysis on wild-type (WT) and NeuroD2 KO cortical cultures to identify potential candidate target genes responsible for any observed changes in cellular electrophysiology. Using this parallel approach we found that NeuroD2 acts in a cell intrinsic manner to regulate neuronal excitability and promote synaptic innervation in developing cortical neurons. By comparing microarray results we identified two transcripts that are significantly decreased in expression in NeuroD2 KO tissue that can mechanistically link NeuroD2 levels to inhibitory synapse number and cellular excitability: gastrin-releasing peptide (GRP) and the small conductance, calcium-activated potassium channel, SK2.

GRP acts on the gastrin-releasing peptide receptor (GRPR) to promote inhibitory neurotransmission (Cao *et al.* 2010). We found GRP mRNA was strongly decreased in NeuroD2 null neurons and the GRPR antagonist RC-3059 partially blocked the increase in inhibitory synaptic inputs onto NeuroD2 over-expressing cells. The small conductance calcium-activated potassium channel, SK2, which is also developmentally regulated (Gymnopoulos *et al.* 2014), regulates intrinsic excitability of neurons by mediating action potential (AP) after-hyperpolarization (Garcia-Junco-Clemente *et al.* 2013). SK2 mRNA was also significantly decreased in the absence of NeuroD2 and NeuroD2 overexpression altered AP parameters in a manner consistent with increased SK2 expression. Moreover, these changes were partially blocked by the SK2 selective antagonist apamin. In brief, our data reveal that the activity-dependent transcription factor NeuroD2 functions as a critical mediator of both neuronal excitability and synaptic innervation during cortical circuit development. Furthermore, NeuroD2 mediates these changes, at least in part, by contributing to the expression of SK2 and GRP.

Methods

Animal care and use

All experimental procedures were performed in accordance with the policies and recommendations of the International Association for the Study of Pain, and have been approved by the Institutional Animal Care and Use Committee of Tulane University, which is a fully AAALAC

© 2016 The Authors. The Journal of Physiology © 2016 The Physiological Society

accredited institute. All efforts were made to minimize the number of animals used for study.

Neuronal cultures

Dissociated cortical neurons were harvested from timed-pregnant embryonic day (E)18 rats or E16 mice. Briefly, for rat cortical cultures, a time-pregnant animal was deeply anaesthetized with isoflurane and killed by cervical dislocation. Embryos were dissected in ice-cold Hanks' balanced salt solution buffer. Cortical caps were dissected (hippocampi removed) and then digested with trypsin for 20 min at 37°C before trituration. Multiple embryos were combined for plating into individual cultured wells, and thus individual cultured coverslips represented multiple animals of unspecified sex. Dissociated neurons were cultured on tissue culture dishes or glass coverslips coated with poly-D-lysine and laminin (BD Biosciences, San Jose, CA, USA). Rat neuron culture medium consisted of basal medium Eagle with 1× Glutamax, 1000 U ml^{-1} penicillin G and streptomycin sulfate, 5% FBS, 1 × N2 supplement and 25 μM β-mercaptoethanol (Invitrogen, Carlsbad, CA, USA). Cultures were maintained at 37°C in 5% ambient CO_2. Media were changed every other day. Mouse cultures were prepared using the same dissection and plating protocols, but with the following growth medium: Neurobasal Medium with 1 × Glutamax, 2% fetal bovine serum, 1 × B27 supplement, and 25 μm β-mercaptoethanol (Invitrogen). Detailed protocols can be found in Hall *et al.* (2007).

Plasmids and transfection

Mouse NeuroD2 cNDA was cloned into the pCS2+ plasmid under control of a CMV promoter (Wilke *et al.* 2012). To generate NeuroD2 shRNA the sequence corresponding to nucleotides 911 to 931 of rat NeuroD2 (GCTCTGTCTCAACGGCAACTT) was cloned into the pLKO.1 expression vector (Wilke *et al.* 2012). Mouse and rat NeuroD2 are 100% conserved in this target region. Cultured neurons were transfected at 8 days *in vitro* (DIV) using Lipofectamine 2000 (Invitrogen). An enhanced green fluorescent protein (eGFP) expressing plasmid (pBos) was used as a transfection marker in all experiments, including control (GFP alone). Positive transfected neurons were confirmed to be excitatory pyramidal neurons by the lack of glutamic acid decarboxylase 65 (GAD65) staining (data not shown).

RNA isolation, microarray analysis and qPCR

RNA was isolated using the RNeasy Mini Kit (Qiagen, Valencia, CA, USA). For microarray analysis, seven samples for each WT and KO mouse cortical cultures were prepared and hybridized to SurePrint G3 mouse GE 8 × 60 K arrays (Agilent, Santa Clara, CA, USA). Array data were processed and analysed similarly to published protocols (Han & Jones, 2014). GeneSpring GX software version 12 (Agilent) was used to analyse microarray data. A probe was selected if it met the following criteria: fold change more than 1.2 and significance $P < 0.05$ with Student's unpaired t test. False discover rates (FDR) were calculated using Benjamini–Hochberg multiple testing correction in Genespring software (presented in Table 1). Two FDR values are reported for each gene, FDR Select and FDR Total. To get values for FDR Select, ∼600 genes, which had fold change > 1.2 and significance $P < 0.05$, were assessed using Benjamini–Hochberg multiple testing correction. For FDR Total, total probes (∼60 K on chip) were assessed using Benjamini–Hochberg multiple testing correction, without cut-off for fold change (= 1.0) nor significance ($P = 1.0$). Gene expression changes were then tested for biological significance using qPCR analysis (Table 1).

For qPCR, 1 μg RNA was harvested from WT and KO mouse cultures and reverse transcribed with iScript cDNA Synthesis kit (Bio-Rad, Hercules, CA, USA). cDNA was subsequently used for real-time quantitative PCR performed in an iCycler Optical Module (Bio-Rad) using SsoFast EvaGreen Supermix (Bio-Rad). Technical replicates as well as no template and no RT negative controls were included and each individual experiment was performed in triplicate samples. Expression of the gene of interest was normalized to *ActinB*. The sequences of the primers used were: *ActinB*, F: 5′-CCACACCCGCCAC-CAGTTCG-3′, R: 5′-CTAGGGCGGCCCACGATGGA-3′; NeuroD2 F: 5′-CAAGAAGCGCGGGCCGAAGA-3′, R: 5′-TTGGCCTTCTGTCGCCGCAG-3′; GRP F: 5′-GTC-ACTGGGCTGTGGGACACTTA-3′, R: 5′-CTTCCCAGC-GGACGTACCCC-3′; SK2 F: 5′-GTCGCTGTATTCTTTA-GCTCTG-3′, R: 5′-ACGCTCATAAGTCATGGC-3′.

Immunohistochemistry

Primary antibodies used were against GAD65 (mouse, 1:1000, Chemicon, MilliporeSigma, St. Louis, MO, USA) and the $GABA_AR\gamma2$ subunit (rabbit, 1:500, Chemicon). Secondary antibodies were Alexa Fluor 594 and 633-conjugated (1:1000, Invitrogen). Cultured neurons were fixed with 4% paraformaldehyde and 2% sucrose in phosphate buffered saline (PBS) for 15 min at room temperature. Cultures were then blocked in 1× blocking buffer (1× PBS, 0.1% Triton X-100, 5% normal donkey serum), incubated with primary antibody in blocking buffer overnight at 4°C and incubated with the secondary antibody in blocking buffer for 1 h at room temperature. Images (1024 × 1024 pixels) were acquired on a Nikon A1 confocal microscope with a

© 2016 The Authors. The Journal of Physiology © 2016 The Physiological Society

Table 1. Selected genes that are downregulated (>1.2-fold) in NeuroD2 KO *vs*. WT cortical tissue

Gene symbol	Fold change	*P*	FDR (Select)	FDR (Total)	Description
Neurod2†‡	−8.81	9.41×10^{-11}	1.78×10^{-8}	5.25×10^{-6}	Neurogenic differentiation factor 2
Grp†‡	−2.48	0.008090833	0.02335726	0.7937901	Gastrin releasing peptide
Kif6	−1.77	0.039458968	0.04267144	0.85842603	Kinesin family member 6
Kcns3	−1.69	0.025873655	0.035351716	0.79384476	Voltage-gated channel, delayed-rectifier, subfamily S, member 3
Plxndl†‡	−1.48	0.005626001	0.016380074	0.7004802	Plexin Dl
Kcnd3	−1.42	0.002585986	0.011132563	0.5020108	Voltage-gated channel, Shal-related family, member 3
Epha6	−1.42	0.002643762	0.011132563	0.6172144	Eph receptor A6
Nefm†	−1.42	0.007119948	0.02335726	0.7937901	Neurofilament, medium polypeptide
Gabra2†	−1.41	0.032407083	0.03593437	0.79715264	GABA-A receptor, subunit α2
Kcnt2	−1.39	0.001616994	0.009913773	0.15403655	Potassium channel, subfamily T, member 2
Foxo6	−1.39	0.043240737	0.045719594	0.8979501	Forkhead box O6
Kcnip4	−1.37	0.002442279	0.010243218	0.41595492	Kv channel interacting protein 4
Kcnjll	−1.37	0.034641597	0.038337044	0.8065073	Potassium inwardly rectifying channel, subfamily J, member 11
Stxbp5l	−1.37	0.048574124	0.04882949	0.95340574	Syntaxin binding protein 5-like
Gabbr2	−1.35	0.006926423	0.019712156	0.7937901	GABA-B receptor, 2
Dixdcl†‡	−1.35	0.01726422	0.031362873	0.7937901	DIX domain containing 1
Foxol	−1.34	0.002442279	0.010243218	0.49281004	Forkhead box O1
Camk2a†	−1.33	0.042989478	0.045495648	0.8933901	Calcium/calmodulin-dependent protein kinase II α
Ppplrlb	−1.32	0.00460536	0.012099204	0.63865095	Protein phosphatase 1, regulatory (inhibitor) subunit 1B
Ephb6	−1.32	0.005699302	0.016380074	0.7109885	Eph receptor B6
Kcnk4	−1.31	0.005386524	0.016380074	0.6707512	Potassium channel, subfamily K, member 4
Atp2bl	−1.31	0.007285039	0.02335726	0.7937901	ATPase, Ca^{2+} transporting, plasma membrane 1
Bok	−1.31	0.021214584	0.034998067	0.7937901	BCL2-related ovarian killer protein
Sla	−1.3	0.04818842	0.04882949	0.92200255	Src-like adaptor
Slitrk3	−1.29	0.03366219	0.036189463	0.8025127	SLIT and NTRK-like family, member 3
Kcncl	−1.29	0.041096598	0.045084268	0.88167274	Potassium voltage-gated channel, Shaw-related subfamily, member 1
Cplx2†‡	−1.28	0.008529506	0.02335726	0.7937901	Complexin 2
Ier5	−1.28	0.012563508	0.030142762	0.7937901	Immediate early response 5
Arrdc2	−1.28	0.012955907	0.030538168	0.7937901	Arrestin domain containing 2
Itprl	−1.28	0.013064444	0.0312032	0.7937901	Inositol 1,4,5-trisphosphate receptor 1
Nrxnl	−1.28	0.024665145	0.035351716	0.7937901	Neurexin I
Grin2c	−1.28	0.03399089	0.036776014	0.8042854	Glutamate receptor, ionotropic, NMDA2C
Mylip	−1.27	0.021410765	0.035166554	0.7937901	Myosin regulatory light chain interacting protein
Ptpn21	−1.26	0.037434865	0.042422105	0.85433745	Protein tyrosine phosphatase, non-receptor type 21
Camk4†	-1.25	0.002294663	0.010165026	0.32551256	Calcium/calmodulin-dependent protein kinase IV
Kcnh3	−1.25	0.004905365	0.012099204	0.6438913	Potassium voltage-gated channel, subfamily H (eag-related), member 3
Cacnala	−1.24	0.010805262	0.02335726	0.7937901	Calcium channel, voltage-dependent, P/Q type, α1A subunit
Klf5	−1.24	0.03539486	0.038420103	0.8133888	Kruppel-like factor 5
Kcnj9	−1.24	0.03978704	0.044782665	0.8609039	Potassium inwardly rectifying channel, subfamily J, member 9
Slc2a6	−1.23	0.020900369	0.034003094	0.7937901	Solute carrier family 2 (facilitated glucose transporter), member 6

(*Continued*)

© 2016 The Authors. The Journal of Physiology © 2016 The Physiological Society

Table 1. Continued

Gene symbol	Fold change	*P*	FDR (Select)	FDR (Total)	Description
Efna5	−1.23	0.03539486	0.03897731	0.82933736	Ephrin A5
Chka	−1.23	0.036945086	0.040957764	0.8425187	Choline kinase α
Ppp2r5b	−1.22	0.01254365	0.02633919	0.7937901	Protein phosphatase 2, regulatory subunit B
Epha4	−1.22	0.017394949	0.032909703	0.7937901	Eph receptor A4
Phactr2	−1.22	0.027841333	0.035731114	0.79680043	Phosphatase and actin regulator 2
Kcnc3	−1.22	0.046944622	0.047048863	0.91154444	Potassium voltage-gated channel, Shaw-related subfamily, member 3
Scnlb	−1.22	0.049731918	0.049957633	0.99979216	Sodium channel, voltage-gated, type I, β
Pik3r6	−1.21	0.012251093	0.023756737	0.7937901	Phosphoinositide-3-kinase, regulatory subunit 6
Npdcl	−1.21	0.03686852	0.03927016	0.8302656	Neural proliferation, differentiation and control gene 1
Stxbp5	−1.21	0.048574124	0.049407627	0.99979216	Syntaxin binding protein 5
Kcnn2†‡	−1.2	9.04×10^{-4}	0.005928889	0.068098344	Potassium intermediate/small conductance calcium-activated channel
Bai2	−1.2	0.006960979	0.021744039	0.7937901	Brain-specific angiogenesis inhibitor 2
Ppmlf	−1.2	0.036424253	0.03927016	0.8300124	Protein phosphatase 1F
Pddcl	−1.2	0.04594794	0.047048863	0.9028201	Parkinson disease 7 domain containing 1
Lrfn5	−1.2	0.04753913	0.0478091	0.91255474	Leucine rich repeat and fibronectin type III domain containing 5
Gcat	−1.2	0.04825415	0.04882949	0.938082	Glycine C-acetyltransferase

Over 50 genes were selected, based on their possible involvement in central nervous development from a list of over 600 probes whose expression was decreased in microarray between NeuroD2 WT and KO with a significant fold change larger than 1.2. Seven pairs of WT and KO culture tissues were included in the microarray analysis. †Genes whose expression we further assessed by qPCR; ‡genes whose change in expression was verified by qPCR (6/10).

60× objective. For each set of antibodies in individual experiments, images were acquired with identical settings for laser power, detector gain, amplifier offset and pinhole diameter. Inhibitory synapse number was quantified following published protocols (Lin *et al.* 2008).

Acute brain slice preparation and electrophysiology

Pups (P13–16) from NeuroD2 WT and KO littermates were anaesthetized with isoflurane and rapidly decapitated. Brains were removed and immediately placed into ice-cold artificial cerebrospinal fluid (ACSF) containing (mM): 124 NaCl, 4 KCl, 26 $NaHCO_3$, 1.26 NaH_2PO_4, 6 $MgCl_2$ and 1 $CaCl_2$ and bubbled with 95% O_2–5% CO_2. Coronal slices 350 μm thick were obtained using a Leica VT1200 vibrating blade microtome. Slices were transferred to an incubation chamber containing bicarbonate-buffered ACSF containing 3 mM $MgCl_2$ and 2 mM $CaCl_2$ and bubbled with 95% O_2–5% CO_2. All recordings were performed at room temperature. TTX 0.5 μM was included to record miniature currents. Whole-cell pipette solution for mIPSC voltage-clamp recordings contained (mM): 120 CsCl, 30 Hepes, 2 $MgCl_2$, 1 $CaCl_2$, 11 EGTA, and 4 ATP (Haam *et al.* 2014). For mEPSC recordings, the internal solution contained (mM): 10 CsCl, 105 $CsMeSO_3$, 0.5 ATP, 0.3 GTP, 10 Hepes, 5 glucose, 2 $MgCl_2$ and 1 EGTA (Hall *et al.* 2007). To record mEPSCs and mIPSCs from the same neurons, internal solution contained (mM): 20 KCl, 100 $CsMeSO_3$, 10 Hepes, 4 ATP, 0.3 GTP, 10 sodium phosphocreatine and 3 QX-314 (Maffei and Turrigiano, 2008). Reversal potentials (−49 mV for GABAergic currents and +10 mV for glutamatergic currents) were predicted and then empirically confirmed by isolating mIPSCs or mEPSCs pharmacologically (mIPSC: 20 μM 6,7-dinitroquinoxaline-2,3-dione (DNQX) and 50 μM (2*R*)-amino-5-phosphonovaleric acid (APV); mEPSC: 50 μM picrotoxin) followed by stepping the holding voltage in 5 mV increments around the predicted reversal potentials. For current-clamp recordings, the internal solution contained (mM): 125 potassium gluconate, 8 NaCl, 5 D-glucose, 5 Hepes, 4 ATP, 0.3 GTP, 2 $MgCl_2$ and 1 EGTA (Ince-Dunn *et al.* 2006). The liquid junction potential for each internal solution was calculated in Clampfit (Molecular Devices, Sunnyvale, CA, USA): mIPSC internal solution: 2.7 mV; mEPSC internal solution: 8.7 mV; internal solution for same cell recordings: 20 mV; and internal solution for current-clamp recordings: 10 mV. In presented data the junction potential was only corrected for in same cell recordings. For slice recordings, layer II/III pyramidal neurons in barrel cortex were identified via IR DIC

© 2016 The Authors. The Journal of Physiology © 2016 The Physiological Society

visualization. Pipette resistances ranged from 4 to 7 MΩ. Access resistance ranged from 8 to 20 MΩ and was monitored for consistency; for analysed cells change was never > 20%. Data were acquired using LabChart software (ADInstruments, Sydney, Australia) or Igor software (Wavemetrics, Lake Oswego, OR, USA) (digitization at 10 kHz and filtering at 2 kHz). Recordings were discarded if the initial leak current was above 300 pA or changed by more than 20% over the course of recording.

Statistics

Data are presented as means ± SD. For microarray and qPCR experiments, expression levels were normalized to WT and tested using Student's *t*-test. The rest of the data (except for in Fig. 6*D*, *G* and *K*) were nested for analysis using a Linear Mixed Model in IBM SPSS, Statistics 22 (IBM, Armonk, NY, USA). Data in Fig. 6*D*, *G* and *K* were tested with two-way ANOVA using UNIANOVA of General Linear Model in SPSS. Data from culture experiments were nested by individual experiment and individual culture (N) and overall cell number (n). Data from acute slices were nested by animal and cell number (n). Multiple comparisons were corrected by *post hoc* LSD test. $^{*}P < 0.05$, $^{**}P < 0.01$ and $^{***}P < 0.001$.

Results

NeuroD2 promotes inhibitory synapses onto cortical pyramidal neurons *in vitro*

Excitatory synaptic innervation must be countered by inhibitory synapses to maintain proper excitatory/inhibitory (E/I) balance on developing neurons (Eichler & Meier, 2008). Because NeuroD2 can be transactivated by calcium influx, which is an integrated signal of excitatory activity in neurons, we hypothesized that NeuroD2 might help balance excitation by promoting synaptic inhibition. To test if NeuroD2 is involved postsynaptically in maintaining inhibitory synaptic tone, we modified its expression in cultured rat cortical neurons by transfecting with NeuroD2-cDNA (overexpression) or plasmid-based RNAi constructs targeting NeuroD2 (knockdown) (Wilke *et al.* 2012) at 8 days *in vitro* (DIV) and then recording miniature IPSCs (mIPSCs) between 18 and 20 DIV. In all experiments, cells were co-transfected with GFP for identification and compared with GFP-alone expressing control neurons. Overexpression of NeuroD2 significantly increased mIPSC frequency while NeuroD2 knockdown decreased mIPSC frequency (Fig. 1*A–C*, $n = 30$ cells from $N = 8$ multiple embryo-derived individual cultures for GFP, $n = 36$ cells from $N = 11$ for NeuroD2-cDNA and $n = 26$ cells, $N = 9$ for NeuroD2-RNAi; $P = 0.021$ between GFP and NeuroD2-cDNA, $P = 0.004$ between GFP and NeuroD2-RNAi, all in 4 individual experiments). Meanwhile there was a minor change in mIPSC amplitude (Fig. 1*A–C*, $P = 0.012$ between GFP and NeuroD2-cDNA, $P = 0.06$ between GFP and NeuroD2-RNAi). Together these data suggest that NeuroD2 positively regulates inhibitory synapse number onto developing cortical pyramidal neurons.

To support our inference that a change in mIPSC frequency is due to a change in inhibitory synapse number, we used antibodies against GAD65 and GABA receptor to anatomically define inhibitory synapses by measuring colocalization of these markers on GFP transfected pyramidal neurons (Lin *et al.* 2008; Hong *et al.* 2008). As in the electrophysiological recordings, cultured rat cortical neurons were transfected at 8 DIV but then fixed and immunostained between 18 and 20 DIV with antibodies that recognize the presynaptic inhibitory marker GAD65 and the postsynaptic inhibitory marker $GABA_A$ receptor $\gamma 2$ subunit ($GABA_AR\gamma 2$). The number of anatomically defined inhibitory synapses was estimated by measuring the number of co-localized GAD65 and $GABA_AR\gamma 2$ puncta overlapping with the somatic GFP signal. Consistent with the mIPSC data, overexpression of NeuroD2 increased the number of anatomically defined inhibitory synapses while knockdown of NeuroD2 showed only a trend to decrease (Fig. 1*D* and *E*, $n = 36$ cells, $N = 7$ for GFP; $n = 46$ cells, $N = 7$ for NeuroD2-cDNA; $n = 32$ cells, $N = 8$, for NeuroD2-RNAi; $P = 0.008$ between GFP and NeuroD2-cDNA, $P = 0.15$ between GFP and NeuroD2-RNAi, all from 3 independent experiments).

NeuroD2 promotes inhibitory synapses through regulation of GRP expression

In parallel experiments, we employed microarray analysis in an attempt to identify gene targets of NeuroD2 transcription that might be involved in synapse development. Interestingly, in our microarray screen performed at 14 DIV on cultured NeuroD2 WT and KO mouse cortical neurons, we found that gastrin-releasing peptide (GRP) was one of the strongest affected mRNAs in terms of fold change, being significantly decreased in NeuroD2 KO neuronal cultures compared to WT control cultures (Table 1). This decrease in GRP mRNA was confirmed by qPCR analysis (Fig. 1*F*, $n = 7$ samples for each WT and KO mouse cultures in microarray, $P = 0.001$; *t* test and $n = 3$ samples, each sample run in triplicate, for each WT and KO mouse cultures in qPCR, $P = 0.002$). We also observed a decrease in GRP mRNA in cortical tissue taken from P14 KO animals compared to WT littermates (WT = 1 ± 0.05 *vs.* KO = 0.66 ± 0.1;

© 2016 The Authors. The Journal of Physiology © 2016 The Physiological Society

mean ± SD, $P = 0.02$). GRP has a positive effect on inhibitory neurotransmission through activation of its receptor GRPR (Shumyatsky *et al.* 2002; Cao *et al.* 2010). To test the involvement of GRP-GRPR in mediating the effects of NeuroD2 overexpression in regulating inhibitory synaptic tone, we used the GRPR antagonist RC-3095 (2 μM) (Shumyatsky *et al.* 2002). Chronic incubation (8–18 DIV) with RC-3059 partially reversed the increase in mIPSC frequency in NeuroD2 overexpressing cultured rat cortical neurons, supporting the hypothesis that the GRP-GRPR system is involved downstream of NeuroD2 to regulate inhibitory synapse development (Fig. 1*G–I*, $n = 8$ cells for GFP, $n = 14$ cells for NeuroD2-cDNA and $n = 11$ cells for NeuroD2-cDNA+RC-3095, $N = 2$–4 for each condition; $P = 0.0008$ between GFP and NeuroD2-cDNA, $P = 0.02$ between NeuroD2-cDNA and NeuroD2-cDNA+RC-3095). Interestingly, RC-3059 alone did not decrease mIPSC frequency significantly in control neurons (data not shown), suggesting that basal activity of GRP-GRPR signalling is low in cultured cortical neurons and that it needs to be activated or enhanced, such as under NeuroD2 overexpressing conditions, in order to see an effect.

In vivo deletion of NeuroD2 decreases frequency of inhibitory and excitatory quantal neurotransmission

To confirm that NeuroD2 also regulates inhibitory synapse development *in vivo*, we generated acute brain slices from a NeuroD2 KO mouse line (Olson *et al.* 2001) and recorded mIPSCs *ex vivo* from layer II/III cortical neurons in somatosensory barrel cortex at postnatal day (P)13–16. Consistent with our *in vitro* knockdown data, we observed a decrease in mIPSC frequency in KO neurons compared to WT neurons in acute brain slices generated from littermate control animals (Fig. 2, $n = 24$ cells for WT and $n = 32$ cells for KO from four pairs of littermate animals; $P = 0.04$). Prior studies demonstrated that excitatory synapse maturation is altered in NeuroD2 KO animals (Ince-Dunn *et al.* 2006; Wilke *et al.* 2012). To determine how loss of NeuroD2 affects synaptic E/I balance in layer II/III neurons, we also recorded mEPSCs from the same brain area in KO and WT animals. We observed a decrease in mEPSC frequency in KO animals compared to WT controls (Fig. 3, $n = 28$ cells for WT and $n = 32$ cells for KO from four pairs of littermate animals, $P = 0.0005$). Because NeuroD2 KO animals are

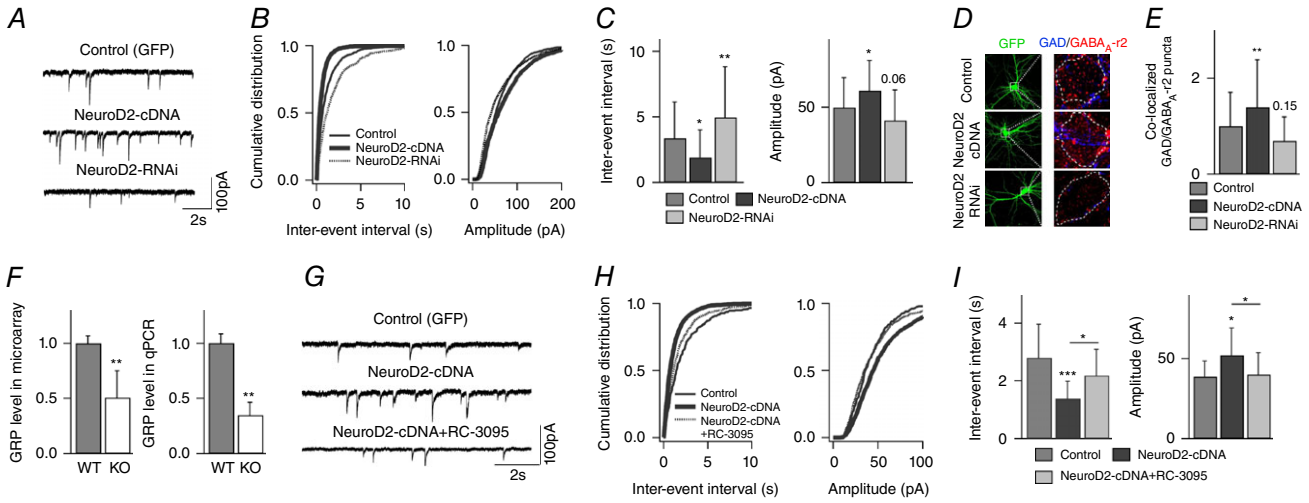

Figure 1. NeuroD2 regulates inhibitory synaptic development through GRP-GRPR signalling *in vitro*
A, representative mIPSCs recorded from cultured cortical neurons transfected with GFP (control), NeuroD2-cDNA or NeuroD2-RNAi plasmid. Scale bar, 100 pA, 2 s. *B*, cumulative distributions of mIPSC inter-event intervals and amplitudes from neurons under the same conditions as in *A*. *C*, summary of mIPSC inter-event intervals and amplitudes from neurons under the same conditions as in *A* ($n = 30$ for GFP, $n = 36$ for NeuroD2-cDNA and $n = 26$ for NeuroD2-RNAi. $^*P < 0.05$; $^{**}P < 0.01$). *D*, representative images of immunofluorescent labeling of GAD65 and GABA$_A$-γ2 in control, NeuroD2-cDNA or NeuroD2-RNAi neurons. *E*, summary of inhibitory synaptic puncta analysis in control, NeuroD2-cDNA or NeuroD2-RNAi neurons ($n = 36$ for GFP, $n = 46$ for NeuroD2-cDNA and $n = 32$ for NeuroD2-RNAi, $^{**}P < 0.01$). *F*, GRP mRNA levels measured by microarray ($n = 7$ for both WT and KO) and by qPCR ($n = 3$ experiments each in triplicate format for both WT and KO) in 14 DIV cultured cortical neurons ($^{**}P < 0.01$). *G*, representative mIPSCs recorded from cultured cortical neurons transfected with GFP and NeuroD2-cDNA in a separate set of experiments. The GRPR antagonist RC-3095 was added into the growth medium after transfection (scale bar, 100 pA, 2 s). *H*, cumulative distributions of mIPSC inter-event intervals and amplitudes recorded from neurons transfected with GFP, NeuroD2-cDNA or NeuroD2-cDNA+RC-3095. *I*, summary of mIPSC inter-event intervals and amplitudes recorded from neurons transfected with GFP, NeuroD2-cDNA or NeuroD2-cDNA+RC-3095 ($n = 8$ for GFP, $n = 14$ for NeuroD2-cDNA and $n = 11$ for NeuroD2-cDNA+RC-3095; $^*P < 0.05$, $^{***}P < 0.001$).

© 2016 The Authors. The Journal of Physiology © 2016 The Physiological Society

prone to seizures, suggestive of an increased E/I ratio, such a compensatory decrease in excitatory transmission in KO animals would not necessarily be predicted. Thus, we wanted to examine this question further.

Since these mEPSC and mIPSC measurements are mean values across many cells and may not properly reflect the absolute E/I balance onto individual neurons, we also measured E/I synaptic balance at the level of individual cortical neurons. To do this we recorded mIPSCs and mEPSCs from single somatosensory layer II/III pyramidal neurons in brain slices by changing the holding potential in voltage-clamp between the reversal potentials for inhibitory and excitatory synaptic currents (−49 mV and +10 mV, determined empirically, see Methods) to isolate excitatory and inhibitory currents, respectively. Interestingly, we observed a similar effect at the single cell level, which was a decrease in both mIPSC and mEPSC frequency (Fig. 4*A–E*, $n = 11$ cells for WT and $n = 13$

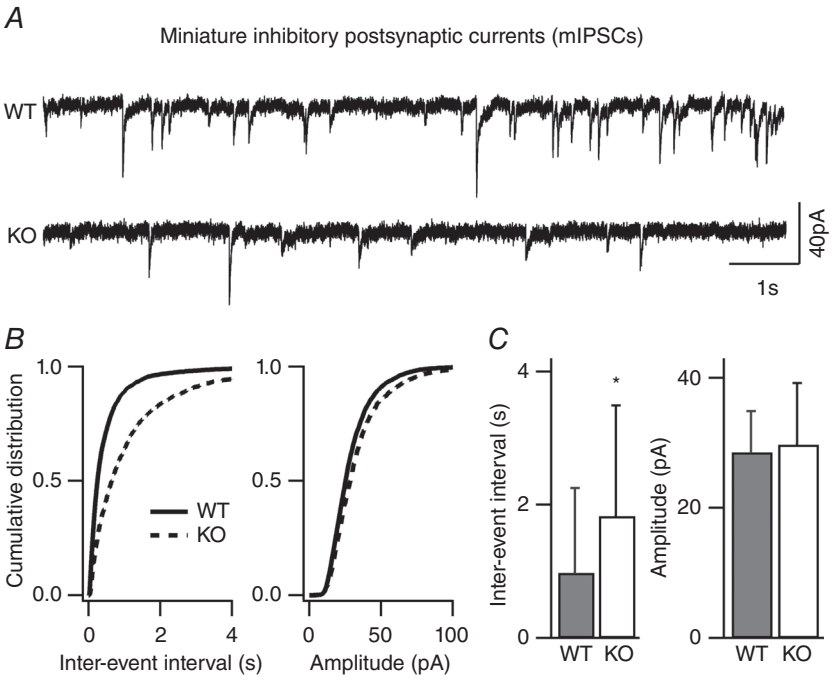

Figure 2. Reduced frequency of inhibitory quantal transmission in layer II/III pyramidal neurons of NeuroD2 null mice
mIPSCs recorded from layer II/III pyramidal neurons in the presence of TTX, APV, and DNQX. *A*, sample traces from WT and mutant neurons voltage clamped at −70 mV (scale bar, 40 pA, 1 s). *B*, cumulative distributions of inter-event interval (IEI) and amplitude from all mIPSCs events of 24 WT neurons and 32 mutant neurons showed a significant rightward shift in the mIPSC frequency for mutant neurons. *C*, average data of mIPSC inter-event intervals and amplitudes showed a significant decrease in mIPSC frequency (increased IEI) in KO neurons ($n = 24$ for WT and $n = 32$ for KO; $^{*}P < 0.05$).

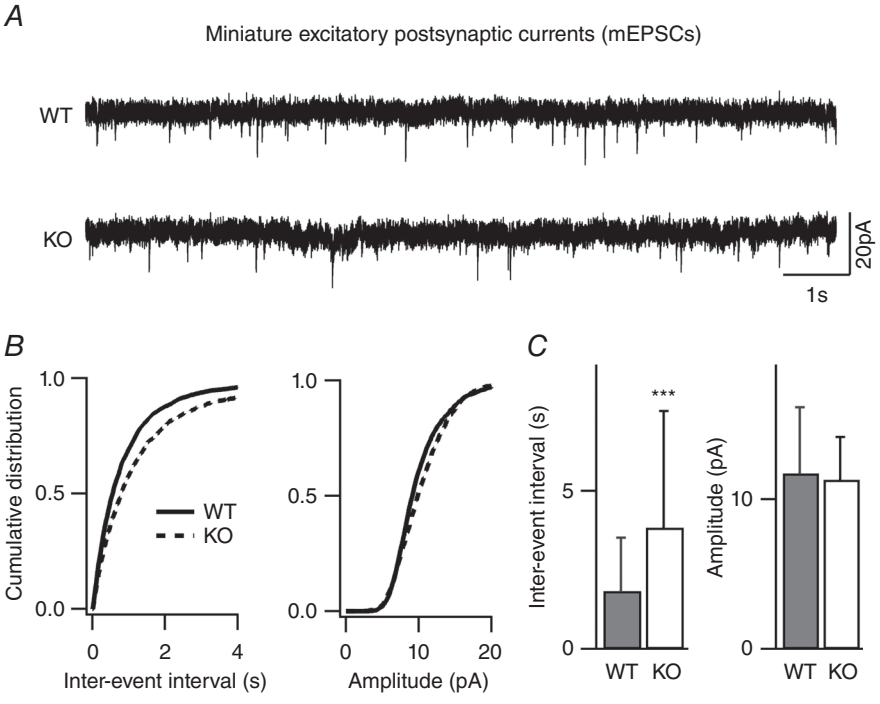

Figure 3. Reduced frequency of excitatory quantal transmission in layer II/III pyramidal neurons of NeuroD2 null mice
mEPSCs recorded from layer II/III pyramidal neurons in the presence of TTX, and picrotoxin. *A*, sample traces from WT and mutant neurons voltage clamped at −65 mV (scale bar, 20 pA, 1 s). *B*, cumulative distributions of inter-event interval and amplitude from all mEPSCs events of 28 WT neurons and 32 mutant neurons showed a significant rightward shift in the mEPSC frequency for mutant neurons. *C*, average data of mEPSC inter-event intervals and amplitudes showed a significant decrease in mEPSC frequency (increased IEI) in KO neurons ($n = 28$ for WT and $n = 32$ for KO; $^{***}P < 0.001$).

© 2016 The Authors. The Journal of Physiology © 2016 The Physiological Society

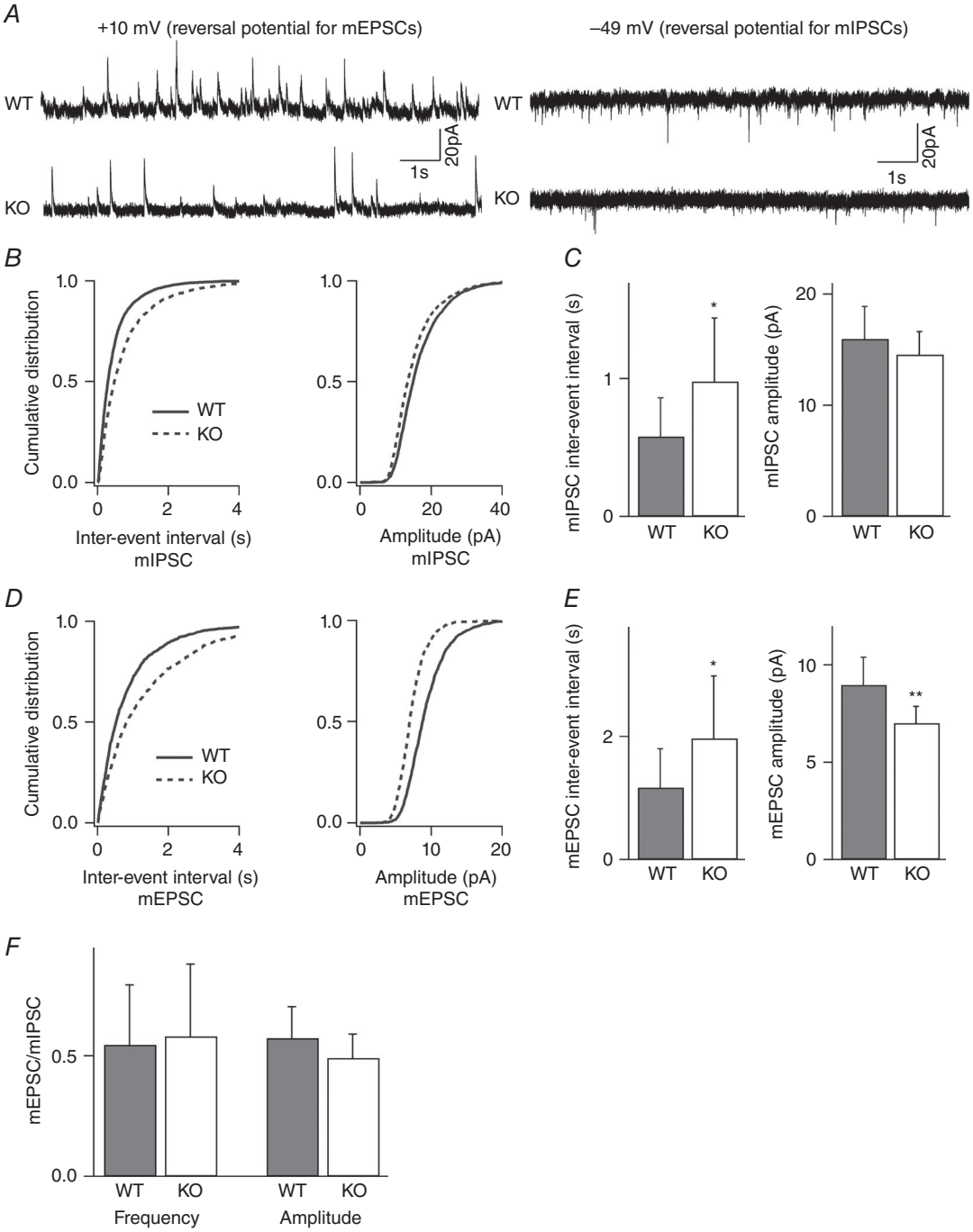

Figure 4. Frequency of both inhibitory and excitatory quantal events is reduced in layer II/III pyramidal neurons of NeuroD2 null mice

mIPSCs and mEPSCs recorded from the same layer II/III pyramidal neurons in the presence of TTX. *A*, sample traces from WT and mutant neurons voltage clamped at +10 mV for mIPSCs and −49 mV for mEPSCs (scale bar, 20 pA, 1 s). *B*, cumulative distributions of inter-event interval and amplitude from all mIPSCs events of 11 WT neurons and 13 mutant neurons showed a significant rightward shift in the mIPSC frequency for mutant neurons. *C*, average data of mIPSC inter-event intervals and amplitudes showed a significant decrease in mIPSC frequency (increased IEI) in KO neurons ($n = 11$ for WT and $n = 13$ for KO; $^{*}P < 0.05$). *D*, cumulative distributions of inter-event interval and amplitude from all mEPSCs events of 11 WT neurons and 13 mutant neurons showed a significant rightward shift in the mEPSC frequency and a leftward shift in the mEPSC amplitude for mutant neurons. *E*, average data of mEPSC inter-event intervals and amplitudes showed a significant decrease in mEPSC frequency (increased IEI) and amplitude in KO neurons ($n = 11$ for WT and $n = 13$ for KO; $^{*}P < 0.05$, $^{**}P < 0.01$). *F*, the ratio of mEPSC to mIPSC IEI and amplitude was unchanged in NeuroD2 mutant neurons compared to WT.

© 2016 The Authors. The Journal of Physiology © 2016 The Physiological Society

cells for KO recorded from two pairs of littermate animals; $P = 0.02$ for mIPSC frequency comparison and $P = 0.04$ for mEPSC comparison). To determine whether there is an overall change in E/I balance in NeuroD2 KO neurons compared to WT neurons, we also calculated an E/I ratio based upon both frequency and amplitude values and saw no difference between NeuroD2 WT and KO neurons (Fig. 4*F*, $P = 0.76$ for E/I ratio in frequency, $P = 0.07$ for E/I ratio in amplitude).

In vivo deletion of NeuroD2 does not alter spontaneous neurotransmission measured *ex vivo*

The data above clearly suggest that inhibitory synapse number is decreased in the absence of NeuroD2 but that this is matched by a decrease in excitatory synapse number, potentially in a homeostatic manner to maintain E/I input ratio between KO and WT animals. This was surprising to us and seemingly incongruent with evidence from previous studies showing that NeuroD2 KO animals are hyperexcitable and prone to seizures. We next turned to measuring spontaneous neurotransmission, since this is a better indicator of network levels of excitability. We recorded sIPSCs and sEPSCs from single somatosensory layer II/III pyramidal neurons by alternating the holding potential in voltage-clamp between the reversal potentials for inhibitory and excitatory synaptic currents, as before, but in the absence of TTX. Strikingly, we observed no change in either frequency or amplitude of sIPSCs and sEPSCs between NeuroD2 WT and KO neurons (Fig. 5*A–E*, $n = 14$ cells for WT and $n = 13$ cells for KO from two pairs of littermate animals; $P = 0.82$ and $P = 0.87$ for sIPSC frequency and amplitude, respectively, $P = 0.37$ and 0.64 for sEPSC frequency and amplitude, respectively).

NeuroD2 regulates the intrinsic excitability of developing pyramidal neurons

Despite a reduction in frequency of mIPSCs and mEPSCs in NeuroD2 KO neurons, the frequency of sIPSC and sEPSC remained unchanged. Excitability is also controlled by cell-intrinsic parameters, which are not reflected in mEPSC and mIPSC recordings. Therefore, a lack of reduction in spontaneous event frequency could suggest an increase in AP frequency in the network, which is also suggested by a previous report where NeuroD2 KO animals displayed low seizure threshold (Olson *et al.* 2001). To determine whether or not the overall excitability of cortical neurons is altered after the loss of NeuroD2 function, we measured spontaneous action potential firing in somatosensory layer II/III pyramidal neurons in barrel cortex from NeuroD2 KO and WT littermates in acute slices. As layer II/III pyramidal neurons incubated in standard ACSF exhibit very low levels of spontaneous activity, we adopted a modified ACSF recipe which is believed to be more similar to *in vivo* rodent CSF than standard ACSF (Nani *et al.* 2005). This modified ACSF was applied to both WT and KO neurons to assess AP activity between these genotypes. Since these recordings are done under different conditions from the sEPSC/IPSC analysis it is not directly comparable but rather these experiments were meant to measure relative differences in AP firing. AP analysis revealed a significant increase in the mean firing rate of NeuroD2 KO compared with WT neurons (Fig. 6*A* and *B*; $n = 10$ cells for WT and $n = 12$ cells for KO from two pairs of littermate animals; $P = 0.04$). To determine the underlying mechanisms associated with the changes in AP rates in layer II/III pyramidal neurons, we injected a series of 500 ms current steps and recorded the voltage response in current-clamp recording in the presence of pharmacological blockers of excitatory and inhibitory synaptic transmission (APV, DNQX and picrotoxin) (Fig. 6*C*). Voltage responses were plotted against injected current amplitude and revealed that NeuroD2 KO neurons responded more strongly to current steps than WT neurons (Fig. 6*D*; $n = 6$ cells for each WT and KO from two pairs of littermate animals; $P = 0.0003$). Membrane input resistance, calculated from the slope of the subthreshold *I–V* curve, was significantly higher in NeuroD2 KO neurons than WT neurons (Fig. 6*E*, $P = 0.01$). To compare intrinsic excitability between WT and KO neurons, a series of 500 ms depolarizing current steps were injected to elicit AP trains in the presence of synaptic blockers. Although there was no significant difference between WT and KO neurons in many parameters such as resting membrane potential measured after break-in, AP threshold, AP amplitude and half-width amplitude of the first evoked AP of a train, the number of APs evoked as a function of current injected was significantly increased in NeuroD2 KO neurons (Fig. 6*F* and *G*; $P = 0.0007$). Notably, we also observed a significant decrease in the amplitude of the after-hyperpolarization (AHP) following the first AP in NeuroD2 KO neurons compared to WT cells (Fig. 6*H* and *I*; $P = 0.009$). Moreover, the ratio of the half-widths of the second and the third APs relative to the first AP of a train was significantly greater in NeuroD2 KO neurons (Fig. 6*J* and *K*; $P = 0.003$).

NeuroD2 regulates AHP partially through SK2 gene expression

The above changes in AP parameters suggested to us an activity-dependent decrement in repolarization in NeuroD2 null cells. In line with this, we noted in our microarray data that mRNA transcript expression of one member of the small conductance Ca^{2+}-activated K^+ channel subfamily, SK2 (*Kcnn2*), was significantly

© 2016 The Authors. The Journal of Physiology © 2016 The Physiological Society

decreased in NeuroD2 KO cultures. Furthermore, we could confirm this difference by qPCR analysis of mouse cortical cultures (Fig. 7*A*; $n = 7$ samples from each WT and KO mouse cultures for microarray, $P = 0.003$, t test; and $n = 5$ samples from each WT and KO mouse cultures for qPCR, $P = 0.04$). We also observed a strong trend to decreased expression of SK2 in KO P14 animals compared to littermate WT cortex (WT = 1 ± 0.1 *vs.* KO = 0.73 ± 0.04; mean ± SD, $P = 0.06$). To test the hypothesis that NeuroD2 regulates the intrinsic excitability of cortical pyramidal neurons through control of SK2 levels, we introduced NeuroD2-cDNA into cultured cortical neurons and then acutely treated cells with the SK2 specific antagonist apamin (300 nM). As predicted, overexpression of NeuroD2 significantly increased AHP amplitude after the first AP of evoked trains, and this

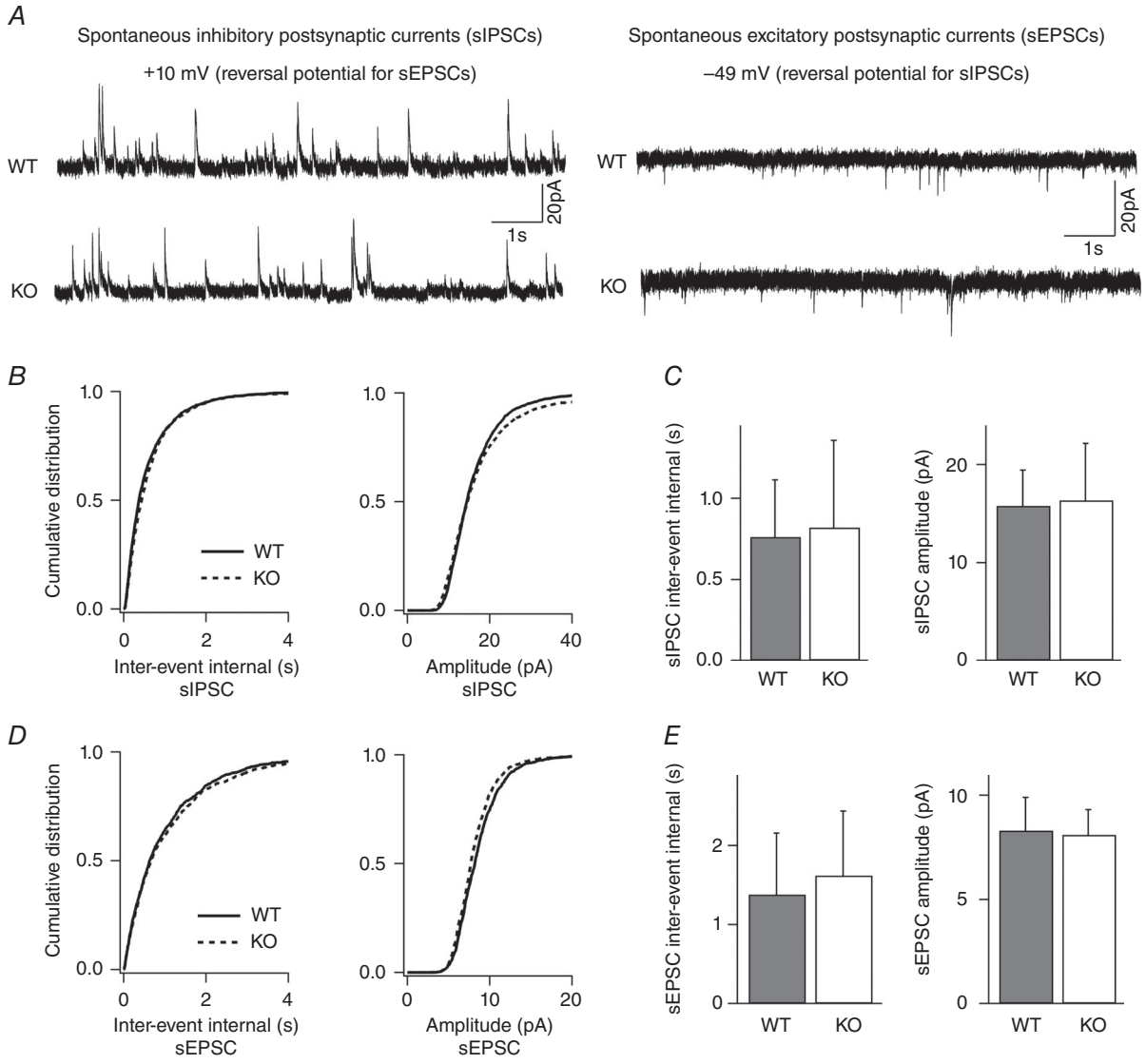

Figure 5. Spontaneous inhibitory and excitatory synaptic neurotransmission in layer II/III pyramidal neurons is unchanged in the absence of NeuroD2
sIPSCs and sEPSCs recorded from single layer II/III pyramidal neurons. *A*, sample traces from a WT and KO neuron voltage clamped at +10 mV for sIPSCs and −49 mV for sEPSCs (scale bar, 20 pA, 1 s). *B*, cumulative distributions of inter-event intervals and amplitudes of all sIPSCs events for 14 WT neurons and 13 KO neurons revealed no difference between WT and mutant neurons. *C*, average data of sIPSC inter-event intervals and amplitudes in WT and mutant neurons ($n = 14$ cells for WT and $n = 13$ cells for KO; $P = 0.82$ and $P = 0.87$ for sIPSC frequency and amplitude, respectively). *D*, cumulative distributions of inter-event intervals and amplitudes from all sEPSC events of 14 WT neurons and 13 mutant neurons showed no difference between WT and mutant neurons. *E*, average data of sEPSC inter-event intervals and amplitudes in WT and mutant neurons ($n = 14$ cells for WT and $n = 13$ cells for KO; $P = 0.37$ and 0.64 for sEPSC frequency and amplitude, respectively).

© 2016 The Authors. The Journal of Physiology © 2016 The Physiological Society

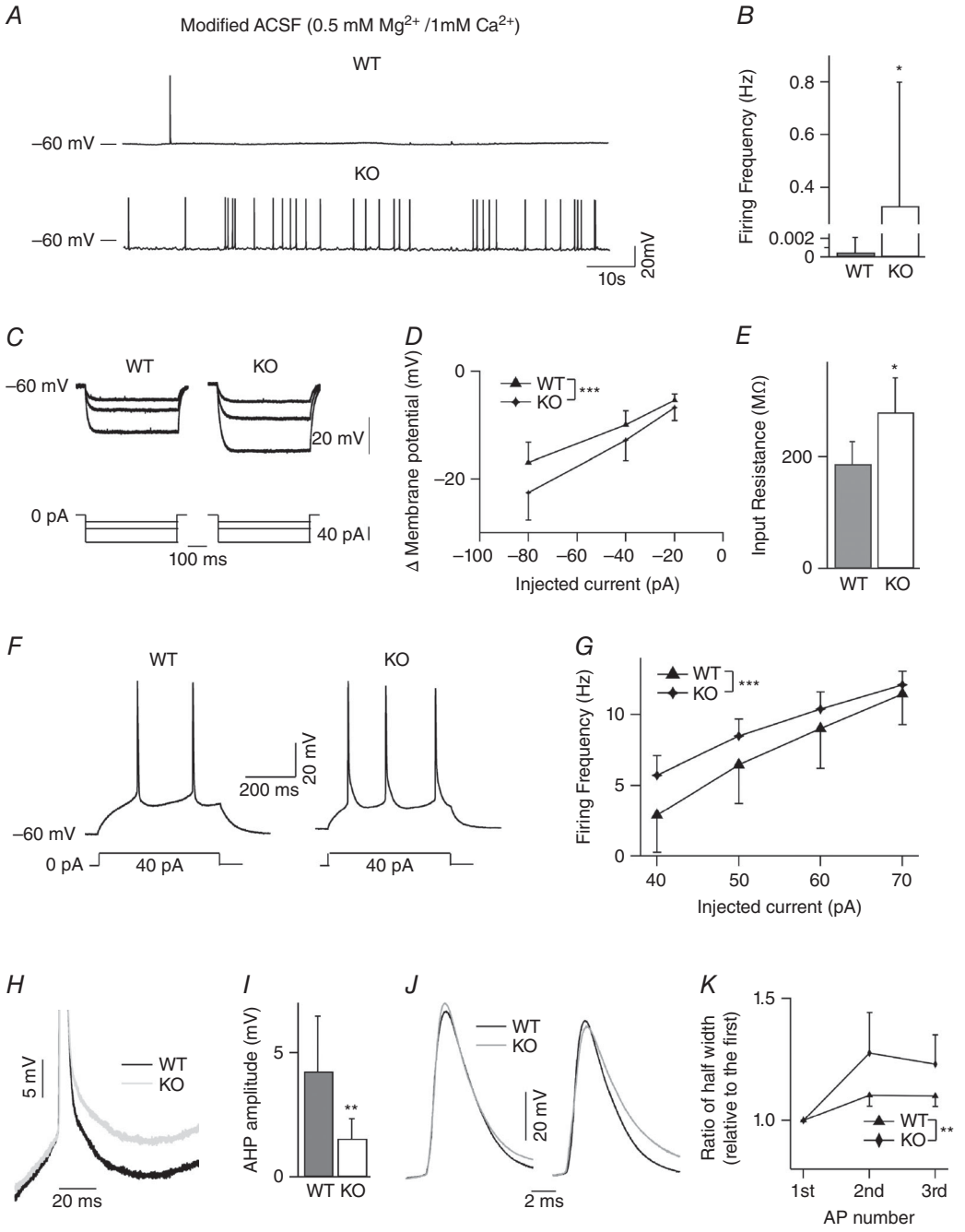

Figure 6. Increased intrinsic excitability and higher spontaneous AP rates in layer II/III pyramidal neurons of NeuroD2 null neurons

A, representative spontaneous AP firing for WT and NeuroD2 null cells. *B*, average spontaneous firing rate was significantly higher in NeuroD2 KO neurons than WT neurons ($n = 10$ for WT and $n = 12$ for KO; $^{*}P < 0.05$). *C*, superimposed voltage traces depicting the response to 500 ms hyperpolarizing step currents in one WT and KO neurons. *D*, current–voltage (*I–V*) curves of the steady-state voltage in relation to injected currents ($n = 6$ for both WT and KO; $^{***}P < 0.001$). *E*, input resistance of mutant neurons was significantly higher than WT neurons ($^{*}P < 0.05$). *F*, example current-clamp recordings in response to 40 pA depolarizing current steps for WT and KO layer II/III cortical neurons. *G*, average firing frequency as a function of the current injected showing an increase in NeuroD2 KO neurons ($n = 6$ for both WT and KO; $^{***}P < 0.001$). *H*, representative traces of AHP after the first AP (in 8 Hz AP trains) in NeuroD2 WT and KO neurons. *I*, average data showed decreased AHP after the first AP in NeuroD2 KO neurons compared to WT neurons ($^{**}P < 0.01$). *J*, representative traces of the first and third APs (in 8 Hz AP trains) from NeuroD2 WT and KO trains shown at expanded time base. *K*, the ratio of the half-widths of the second and the third APs relative to the first AP is significantly greater in the KOs ($^{**}P < 0.01$).

© 2016 The Authors. The Journal of Physiology © 2016 The Physiological Society

was partially dependent on Kcnn2 activity as shown by its sensitivity to apamin (Fig. 7*B* and *C*; $n = 15$ cells for GFP, $n = 11$ cells for NeuroD2-cDNA, and $n = 9$ cells for NeuroD2-cDNA + apamin from $N = 2$–3 for each condition; $P = 0.0001$ between GFP and NeuroD2-cDNA, $P = 0.047$ between NeuroD2-cDNA and NeuroD2-cDNA + apamin). These data suggest that NeuroD2 regulates neuronal AHP, and therefore intrinsic excitability (at least in part) by regulating SK2 gene expression.

Discussion

Our experiments show that NeuroD2 regulates the developmental excitability of cortical pyramidal neurons by influencing both the amount of inhibitory synaptic innervation they receive and their cell-intrinsic excitability. In NeuroD2 KO neurons, we observed a decrease in both excitatory and inhibitory synaptic tone, but also increased cell-intrinsic excitability. Together, these data not only provide insight about the links between synaptic and cell-intrinsic excitability but also clearly point to a critical role for NeuroD2 in coordinating these processes and maintaining proper levels of neuronal excitability in developing cortex.

In addition to describing a role for NeuroD2 in maintaining neuronal excitability, we identified potential gene targets that could be involved mechanistically. Using microarray analysis and qPCR confirmation, we identified GRP and SK2 as transcripts that are decreased in the absence of NeuroD2. Knowledge of the direct transcriptional targets of NeuroD2 in neurons has been lacking and to our knowledge thus far, this is the first evidence of an activity-dependent transcription factor that regulates both synaptic and cell-intrinsic properties of pyramidal neuron development.

Our data suggest that NeuroD2 promotes synaptic inhibition in a manner that requires GRPR activation. GRPR is the receptor for GRP, which is a 29 amino acid-long mammalian homolog of the amphibian peptide bombesin and may serve as a cotransmitter with glutamate in pyramidal neurons in the rodent brain (Lee *et al.* 1999; Shumyatsky *et al.* 2002; Cao *et al.* 2010). GRP expresses across many brain areas including cortex, hippocampus and amygdala (Wada *et al.* 1990), and is required for proper social behaviour (Merali *et al.* 2014), adult neurogenesis (Walton *et al.* 2014) and fear conditioned learning (Bédard *et al.* 2007). GRP released from pyramidal neurons acts on GRPRs expressed on inhibitory neurons to modulate GABAergic vesicle release (Shumyatsky *et al.* 2002). We confirmed that NeuroD2 also expresses exclusively in pyramidal neurons in mouse cortex (data not shown). These data suggest that NeuroD2 supports GRP expression to promote inhibitory synapse number as measured by mIPSC frequency. While mIPSC frequency can reflect a change in synapse number it is also dependent upon presynaptic vesicle release probability. While we did not test inhibitory synapse release probability, our anatomical synapse staining data support the idea that the number of inhibitory synapses onto NeuroD2 null cells is decreased.

As mentioned above, NeuroD2 KO also resulted in a decrease in mEPSC frequency. However, based upon the absence of any obvious regulators of excitatory synapse development on our NeuroD2 KO microarray along with the observations that NeuroD2 overexpression in cultured cortical neurons decrease mEPSC frequency (data not shown) and synaptic scaling is intact in NeuroD2 KO neurons (data not shown), we infer that this may be a compensatory effect, due to a homeostatic plasticity mechanism in response to decreased inhibitory synaptic tone. Despite a decrease in both inhibitory and excitatory

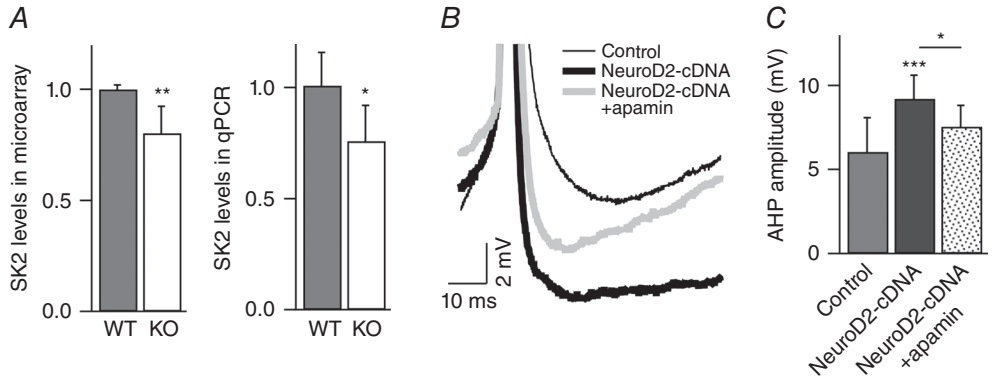

Figure 7. NeuroD2 regulates AHP through SK2
A, SK2 mRNA levels are decreased in NeuroD2 KO tissue as measured by microarray ($n = 7$ for both WT and KO) and qPCR ($n = 5$ experiments with each in triplicate for both WT and KO). Data are from 14 DIV cultured cortical neurons (*$P < 0.05$; **$P < 0.01$). *B*, representative traces of AHP after the first AP (in 8 Hz AP trains) in control, NeuroD2-cDNA, and NeuroD2-cDNA + apamin. *C*, summary of AHP measurements after the first AP in control, NeuroD2-cDNA and NeuroD2-cDNA + apamin (*$P < 0.05$, ***$P < 0.001$).

© 2016 The Authors. The Journal of Physiology © 2016 The Physiological Society

synaptic events, NeuroD2 KO mice have low seizure thresholds when induced by kainic acid (Olson *et al.* 2001). How might a perceived balanced decrease in synaptic E/I input lead to seizure susceptibility? Neurons also regulate their excitability through cell-intrinsic mechanisms, which are developmentally regulated and susceptible to plasticity (Turrigiano, 2011). AP-mediated Ca^{2+} influx opens potassium channels that control AP firing properties. While delayed-rectifier potassium channels are responsible for the majority of repolarization during a single AP, calcium-activated potassium channels determine the degree of AHP and become more dominant during sustained firing (Adelman *et al.* 2012). SK2 (also known as $K_{Ca}2.2$) is encoded by the *KCNN2* gene and is a member of the potassium intermediate/small conductance calcium-activated channel subfamily. It is exclusively activated by intracellular calcium ions and triggers potassium flux to regulate cell-intrinsic excitability. The channel is important for learning and memory and is expressed in neurons across different brain areas including pyramidal neurons in all layers of the cortex (Sailer *et al.* 2004; Gymnopoulo *et al.* 2014). Activation of SK2 channels contributes to AHPs of medium duration (mAHPs) and directly affects neuronal intrinsic excitability. The decreased expression of SK2 in NeuroD2 KO neurons predicts a hyper-excitation phenotype and could contribute to epileptic activity in these animals. In addition, we observed an increase in input impedance in NeuroD2 null neurons. It remains to be determined if this is related to decreased expression of a direct transcriptional target of NeuroD2.

NeuroD2 is a neuronal activity-dependent transcription factor. In our unpublished data we have seen Npas4 expression is increased dramatically following KCl stimulation in WT cortical cultures and that this increase is significantly attenuated in NeuroD2 null cultures. Yet, under conditions of basal activity we observed no difference in Npas4 levels between NeuroD2 KO and WT cultures (data not shown). Moreover, in preliminary experiments we noted that if we knock down Npas4 with a siRNA plasmid in single cortical pyramidal neurons *in vitro*, this can block the ability of NeuroD2 overexpression to increase mIPSC event number (data not shown). Bidirectional manipulation of the activity-dependent transcription factor Npas4 results in similar effects on mIPSC frequency in hippocampal neurons *in vitro*; increased inhibition in response to increased Npas4 levels and decreased inhibitory events following knockdown of Npas4 (Lin *et al.* 2008). It is also of interest to note that Npas4 has been shown to be required for synaptic changes downstream of changes in cell-intrinsic excitability in adult-born neurons (Sim *et al.* 2013). Together these data suggest a complex interaction between Npas4 and NeuroD2. Understanding the relationship and potential coordination of these two transcription factors in regulating synaptic development will be a very interesting avenue for future research.

In summary, our data point to NeuroD2 as a critical regulator of cortical pyramidal neuron excitability, consistent with previously reported increased susceptibility to seizure in the NeuroD2 KO animals. We also found these animals exhibit altered social behavioure (data not shown). The data raise very compelling questions including how other aspects of intrinsic excitability and synaptic innervation are linked. It will be interesting to determine in future experiments what type of inhibition is specifically regulated by NeuroD2 transcription and discover exactly what the mechanism of stabilization is downstream of GRPR activation. Furthermore, are these processes recapitulated in adult-born neurons as it is believed that similar developmental processes must be evoked during circuit integration in the developed brain (Scobie *et al.* 2009) Recent work, published during preparation and review of this article, has used ChIP-seq to identify gene expression changes during embryonic development (E14.5) in NeuroD2 null embryos (Bayam *et al.* 2015). Interestingly, taken together with our results, the data suggest that NeuroD2 may affect expression of different genes depending upon developmental age of neurons. Future studies will be required to determine the answers to these questions and piece together the multiple ways in which cortical pyramidal neurons maintain E/I balance and cell excitability including via regulation of NeuroD2 levels during postnatal synapse formation. A complete understanding of these mechanisms will be critical for understanding autism spectral disorders and epilepsy and thus determining therapeutic interventions.

References

Adelman JP, Maylie J & Sah P (2012). Channels: Form and function. *Annu Rev Physiol* **74**, 245–269.

Bayam E, Sahin GS, Guzelsoy G, Guner G, Kabakcioglu A & Ince-Dunn G (2015). Genome-wide target analysis of NEUROD2 provides new insights into regulation of cortical projection neuron migration and differentiation. *BMC Genomics* **16**, 681

Bédard T, Mountney C, Kent P, Anisman H & Merali Z (2007). Role of gastrin-releasing peptide and neuromedin B in anxiety and fear-related behaviour. *Behav Brain Res* **179**, 133–140.

Cao X, Mercaldo V, Li P, Wu L-J & Zhuo M (2010). Facilitation of the inhibitory transmission by gastrin-releasing peptide in the anterior cingulate cortex. *Mol Pain* **6**, 52.

Eichler SA & Meier JC (2008). E-I balance and human diseases – from molecules to networking. *Front Mol Neurosci* **1**, 2.

Garcia-Junco-Clemente P, Chow DK, Tring E, Lazaro MT, Trachtenberg JT & Golshani P (2013). Overexpression of calcium-activated potassium channels underlies cortical dysfunction in a model of PTEN-associated autism. *Proc Natl Acad Sci USA* **110**, 18297–18302.

© 2016 The Authors. The Journal of Physiology © 2016 The Physiological Society

Gymnopoulos M, Cingolani LA, Pedarzani P & Stocker M (2014). Developmental mapping of small-conductance calcium-activated potassium channel expression in the rat nervous system. *J Comp Neurol* **522**, 1072–1101.

Haam J, Halmos KC, Di S & Tasker JG (2014). Nutritional state-dependent ghrelin activation of vasopressin neurons via retrograde trans-neuronal-glial stimulation of excitatory GABA circuits. *J Neurosci* **34**, 6201–6213.

Hall BJ, Ripley B & Ghosh A (2007). NR2B signaling regulates the development of synaptic AMPA receptor current. *J Neurosci* **27**, 13446–13456.

Han W & Jones FE (2014). HER4 selectively coregulates estrogen stimulated genes associated with breast tumor cell proliferation. *Biochem Biophys Res Commun* **443**, 458–463.

Hoischen A, Krumm N & Eichler EE (2014). Prioritization of neurodevelopmental disease genes by discovery of new mutations. *Nat Neurosci* **17**, 764–772.

Hong EJ, McCord AE & Greenberg ME (2008). A biological function for the neuronal activity-dependent component of Bdnf transcription in the development of cortical inhibition. *Neuron* **60**, 610–624.

Imayoshi I & Kageyama R (2014). bHLH factors in self-renewal, multipotency, and fate choice of neural progenitor cells. *Neuron* **82**, 9–23.

Ince-Dunn G, Hall BJ, Hu S-C, Ripley B, Huganir RL, Olson JM, Tapscott SJ & Ghosh A (2006). Regulation of thalamocortical patterning and synaptic maturation by NeuroD2. *Neuron* **49**, 683–695.

Kohwi M & Doe CQ (2013). Temporal fate specification and neural progenitor competence during development. *Nat Rev Neurosci* **14**, 823–838.

Lee BH, Smith T & Paciorkowski AR (2015). Autism spectrum disorder and epilepsy: Disorders with a shared biology. *Epilepsy Behav* **47**, 191–201.

Lee K, Dixon AK, Gonzalez I, Stevens EB, McNulty S, Oles R, Richardson PJ, Pinnock RD & Singh L (1999). Bombesin-like peptides depolarize rat hippocampal interneurones through interaction with subtype 2 bombesin receptors. *J Physiol* **518**, 791–802.

Lin Y, Bloodgood BL, Hauser JL, Lapan AD, Koon AC, Kim T-K, Hu LS, Malik AN & Greenberg ME (2008). Activity-dependent regulation of inhibitory synapse development by Npas4. *Nature* **455**, 1198–1204.

Maffei A & Turrigiano GG (2008). Multiple modes of network homeostasis in visual cortical layer 2/3. *J Neurosci* **28**, 4377–4384.

McCormick MB, Tamimi RM, Snider L, Asakura A, Bergstrom D & Tapscott SJ (1996). NeuroD2 and neuroD3: distinct expression patterns and transcriptional activation potentials within the neuroD gene family. *Mol Cell Biol* **16**, 5792–5800.

Merali Z, Presti-Torres J, MacKay JC, Johnstone J, Du L, St-Jean A, Levesque D, Kent P, Schwartsmann G, Roesler R, Schroder N & Anisman H (2014). Long-term behavioural effects of neonatal blockade of gastrin-releasing peptide receptors in rats: Similarities to autism spectrum disorders. *Behav Brain Res* **263**, 60–69.

Nani VS, Chang Q, Maffei A, Turrigiano GG, Jaenisch R & Nelson SB (2005). Reduced cortical activity due to a shift in the balance between excitation and inhibition in a mouse model of Rett syndrome. *Proc Natl Acad Sci USA* **102**, 12560–12565.

Olson JM, Asakura A, Snider L, Hawkes R, Strand A, Stoeck J, Hallahan A, Pritchard J & Tapscott SJ (2001). NeuroD2 is necessary for development and survival of central nervous system neurons. *Dev Biol* **234**, 174–187.

Sailer CA, Kaufmann WA, Marksteiner J & Knaus HG (2004). Comparative immunohistochemical distribution of three small-conductance Ca^{2+}-activated potassium channel subunits, SK1, SK2, and SK3 in mouse brain. *Mol Cell Neurosci* **26**, 458–469.

Scobie KN, Hall BJ, Wilke SA, Klemenhagen KC, Fujii-Kuriyama Y, Ghosh A, Hen R & Sahay A (2009). Krüppel-like factor 9 is necessary for late-phase neuronal maturation in the developing dentate gyrus and during adult hippocampal neurogenesis. *J Neurosci* **29**, 9875–9887.

Shumyatsky GP, Tsvetkov E, Malleret G, Vronskaya S, Hatton M, Hampton L, Battey JF, Dulac C, Kandel ER & Bolshakov VY (2002). Identification of a signaling network in lateral nucleus of amygdala important for inhibiting memory specifically related to learned fear. *Cell* **111**, 905–918.

Sim S, Antolin S, Lin CW, Lin Y & Lois C (2013). Increased cell-intrinsic excitability induces synaptic changes in new neurons in the adulte dentate gyrus that require Npas4. *J Neurosci* **33**, 7928–7940

Turrigiano G (2011). Too many cooks? Intrinsic and synaptic homeostatic mechanisms in cortical circuit refinement. *Annu Rev Neurosci* **34**, 89–103.

Wada E, Way J, Lebacq-Verheyden AM & Battey JF (1990). Neuromedin B and gastrin-releasing peptide mRNAs are differentially distributed in the rat nervous system. *J Neurosci* **10**, 2917–2930.

Walton NM, de Koning A, Xie X, Shin R, Chen Q, Miyake S, Tajinda K, Gross AK, Kogan JH, Heusner CL, Tamura K & Matsumoto M (2014). Gastrin-releasing peptide contributes to the regulation of adult hippocampal neurogenesis and neuronal development. *Stem Cells* **32**, 2454–2466.

Wilke SA, Hall BJ, Antonios JK, DeNardo LA, Otto S, Yuan B, Chen F, Robbins EM, Tiglio K, Williams ME, Qiu Z, Biederer T & Ghosh A (2012). NeuroD2 regulates the development of hippocampal mossy fibre synapses. *Neural Dev* **7**, 9.

Additional information

Competing interests

The authors declare no conflict of interest.

Author contributions

F.C.: conception and design; collection and assembly of data; data analysis and interpretation; manuscript writing. J.M.: collection

© 2016 The Authors. The Journal of Physiology © 2016 The Physiological Society

and assembly of data. Y.Z.: collection and assembly of data. K.A.: collection and assembly of data. D.Y.: collection and assembly of data. L.S.: provision of study materials. P.D.: provision of study materials; data analysis and interpretation. F.J.: provision of study materials. B.H.: conception and design; financial support; collection and assembly of data; data analysis and interpretation; manuscript writing. Experiments were performed at Tulane University. All authors have approved the final version of the manuscript and agree to be accountable for all aspects of the work. All persons designated as authors qualify for authorship, and all those who qualify for authorship are listed.

Funding

This work was funded by NIMH R01 (MH099378-01), NSF CAREER Award (0952455) and Brain and Behavior Research Foundation YIA (18996) all to B.J.H.

© 2016 The Authors. The Journal of Physiology © 2016 The Physiological Society